

CLOSURE: Assessing Systematic Generalization of CLEVR Models

Dzmitry Bahdanau^{*12} Harm de Vries¹ Timothy J. O’Donnell⁴ Shikhar Murty⁵

Philippe Beaudoin¹ Yoshua Bengio²³⁶ Aaron Courville²³⁶

¹Element AI ²Quebec Artificial Intelligence Institute (Mila)

³Université de Montréal ⁴McGill University ⁵Stanford University ⁶CIFAR Fellow

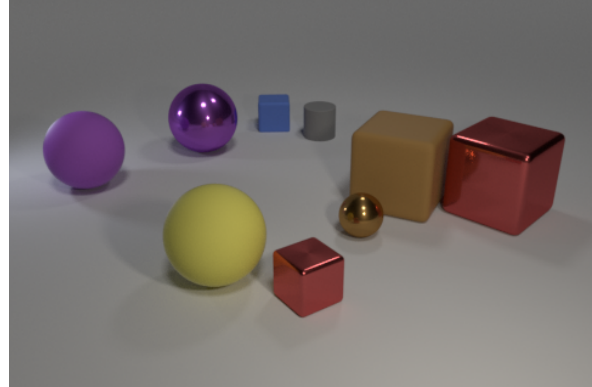
Abstract

The CLEVR dataset of natural-looking questions about 3D-rendered scenes has recently received much attention from the research community. A number of models have been proposed for this task, many of which achieved very high accuracies of around 97-99%. In this work, we study how systematic the generalization of such models is, that is to which extent they are capable of handling novel combinations of known linguistic constructs. To this end, we test models’ understanding of referring expressions based on matching object properties (such as e.g. “another cube that is the same size as the brown cube”) in novel contexts. Our experiments on the thereby constructed CLOSURE benchmark show that state-of-the-art models often do not exhibit systematicity after being trained on CLEVR. Surprisingly, we find that an explicitly compositional Neural Module Network model also generalizes badly on CLOSURE, even when it has access to the ground-truth programs at test time. We improve the NMN’s systematic generalization by developing a novel Vector-NMN module architecture with vector-valued inputs and outputs. Lastly, we investigate how much few-shot transfer learning can help models that are pretrained on CLEVR to adapt to CLOSURE. Our few-shot learning experiments contrast the adaptation behavior of the models with intermediate discrete programs with that of the end-to-end continuous models.

1 Introduction

The ability to communicate in natural language and ground it effectively into our rich unstructured 3D reality is a crucial skill that we expect from artificial agents of the future. A popular task to benchmark progress towards this goal is *Visual Question*

^{*}Work mostly done during PhD studies at Université de Montréal and Mila.



Q1 (CLEVR): There is **another cube that is the same size as the brown cube**; what is its color?

Q2 (CLEVR): There is a thing that is in front of the yellow thing; does it have the same color as cylinder?

Q3 (CLOSURE): There is **another rubber object that is the same size as the gray cylinder**; does it have the same color as the tiny shiny block?

Figure 1: CLEVR questions (Q1 and Q2) require complex multi-step reasoning about the contents of 3D-rendered images. We construct CLOSURE questions (Q3) by using the referring expressions that rely on matching object properties (e.g. the red fragment in Q1) in novel contexts, such as e.g. comparison questions with two referring expressions (Q2).

Answering (VQA), in which one must give a (typically short) answer to a question about the content of an image. The release of the relatively large VQA 1.0 dataset by Antol et al. (2015) ignited the interest for the VQA setup, but researchers soon found that the biases of natural data (such as the heavily skewed answer distribution for certain question types) make it hard to interpret the VQA 1.0 results (Agrawal et al., 2016). To complement biased natural data, Johnson et al. (2016) constructed the CLEVR dataset of complex synthetic questions about 3D-rendered scenes to be free of such biases (see Q1 and Q2 in Figure 1 for examples of CLEVR questions). The CLEVR dataset has spurred VQA modeling research, and many models were designed for it and showcased

decompose the model into components that can be recombined arbitrarily. To improve the NMN’s generalization, we develop a new Vector-NMN module with a vector-valued (as opposed to tensor-valued) inputs and outputs. We show that the Vector-NMN modules perform much better than prior work when assembled in configurations that are different from the training ones. Lastly, we complement our zero-shot systematic generalization analysis with a few-shot transfer learning study and contrast the few-shot adaptation behavior of models with and without symbolic programs.

2 CLOSURE: A Systematic Generalization Benchmark for CLEVR

Analysis of CLEVR The key source of diversity and complexity in CLEVR questions is how objects of interest are referred to. We call a noun phrase a *referring expression* (RE) when it refers to an object or a set of objects, themselves called *referents*. We distinguish three kinds of REs that occur in CLEVR: simple REs, complex REs and logical REs. A *simple RE* is a noun that is (optionally) modified by one or more adjective, e.g. “the big red cube” or “yellow shiny spheres”. In *Complex REs*, a relative clause (in square brackets in all examples below) is used to modify the noun (possibly in addition to adjectives):

the cube [that is left of $\langle RE \rangle$], (1)

big cubes [that are the same color as $\langle RE \rangle$]. (2)

Here, $\langle RE \rangle$ is the *embedded RE*, which can be either simple or also complex. Complex REs in CLEVR can be *spatial* (Example 1) or rely on matching objects’ properties (Example 2). We will call the latter *matching REs*. The RE’s type is determined by whether a *spatial predicate* (“is left of $\langle RE \rangle$ ”, “is right of $\langle RE \rangle$ ”, ...) or a *matching predicate* (“is the same size as $\langle RE \rangle$ ”, “is the same color as $\langle RE \rangle$ ”, ...) is used to construct the relative clause.¹ In *Logical REs*, two REs (Example 3) or two prepositional phrases (Example 4) are combined using “and” or “or”:

[balls] or [red blocks behind the cylinder], (3)

a cylinder that is [left of the brown ball]

and [in front of the tiny block] (4)

¹Note that the original paper by (Johnson et al., 2016) these are called “spatial relationships” and “same-attribute relationships”

The second most important axis of variation in CLEVR is what kind of question is asked about the referents. CLEVR includes existence, counting, attribute and object comparison questions, see examples below:

- (existence) Is there a small cyan object?
- (counting) How many purple things are behind the cylinder?
- (attribute) What material is the big ball?
- (comparison) Do the red thing and the big thing have the same shape?

In existence, counting and attribute questions there is one top-level RE, whereas comparison questions contain two top-level REs.

CLOSURE questions We have constructed the CLOSURE dataset by generating new CLEVR-like questions with matching predicates. To this end, we analyzed the composition of CLEVR and found a number of question templates in which a spatial predicate could be seamlessly substituted for a matching one. We focused on 7 cases where such substitution was possible and where it yielded questions that were not possible under CLEVR’s original data distribution. Below, we describe and give examples of each of the resulting 7 CLOSURE tests. For a more technical explanation of the question generation procedure we refer the reader to Appendix F.

The **embed_spa_mat** test contains existence questions with a matching RE that has an embedded spatial RE, e.g:

- Is there a cylinder that is the same material as the object to the left of the blue thing?

Here, a spatial RE “the object to the left of the blue thing” is embedded in a matching RE “a cylinder that is the same material ...”. Note, that in original CLEVR matching REs can only contain simple embedded REs. A closely related test is **embed_mat_spa**, in which the top-level RE is spatial and the embedded one uses property matching:

- Is there a thing behind the cube that is the same color as the ball?

In **compare_mat** and **compare_mat_spa** tests we focus on models’ ability to understand matching REs in comparison questions:

- There is another small cylinder that is the same material as the small cyan cylinder; does it have the same color as the block?
- There is another cube that is the same material as the gray cube; does it have the same size as the metal thing to the right of the tiny gray cube?

The comparison questions in CLEVR only use spatial REs, hence `compare_mat` and `compare_mat_spa` require models to recombine known constructs (that is the matching REs and the comparison questions) in a novel way. The two tests differ in whether the second RE is simple (`compare_mat`) or spatial (`compare_mat_spa`).

The remaining three CLOSURE tests assess models’ understanding of matching predicates in logical REs. The `or_mat` and `or_mat_spa` questions require counting referents for a logical “or” of two REs, one of which uses property matching:

- How many things are cubes or cylinders that are the same size as the red object?
- How many things are objects that are in front of the blue thing or small metallic things that are the same color as the rubber block?

The `or_mat_spa` test differs from the `or_mat` one in that the second RE is also a complex one. The `and_mat_spa` test contains attribute questions in which the RE involves a logical “and” of a spatial and a matching predicate:

- What is the color of the thing that is to the left of the red cylinder and is the same size as the red block?

All the three tests presented above contain questions that are impossible under CLEVR’s original data distribution, as logical REs in CLEVR only employ spatial predicates.

To construct CLOSURE questions and to compute the ground-truth answers we generated symbolic programs in the functional domain-specific language (DSL) that is CLEVR is based on. See Figure 2 for example programs P1 and P2. Another usecase for groundtruth programs is to bootstrap learning in models that internally use programs as representations of questions’ meanings, such e.g. NMNs. We refer the reader to Appendix A for a description of the DSL and a detailed analysis of how CLOSURE programs differ from the CLEVR ones.

Dataset statistics We release a validation set, a test set and a small training set for few-shot learning investigations. The validation and test sets contain 3600 questions about the respective non-overlapping subsets of CLEVR validation images per each CLOSURE test. The training questions (36 per CLOSURE test) are asked about training images from CLEVR. The data is available at <https://zenodo.org/record/3634090#.Xjc3R3VKi90>

3 Models

We experiment with a number of existing models, as well as with a novel Vector-NMN neural module that we employ in the context of the NMN paradigm. Throughout this section we use capital letters for matrix- or tensor-shaped parameters of all models and small letters for the vector-valued ones. The symbols in equations that are not otherwise defined stand for trainable parameters (in particular this covers weight matrices W, W_1, U, \dots and bias vectors b, b_1, \dots). We use $*$ to denote convolution as well as to inform the reader that the symbols on the left and right sides of the operator are a 4D and a 3D tensor respectively. \odot and \oplus are used to denote feature-wise multiplication and addition for the case where one argument is a 3D tensor and another is a vector. The respective operation is applied independently to all sub-vectors of the tensor-valued argument obtained by fixing its first two indices (the approach known as “broadcasting”). We use square brackets $[x; y]$ to denote tensor concatenation performed along the last axis.

3.1 End-to-End Differentiable Models

The most generic method that we consider is Feature-wise Linear Modulation (FiLM) by Perez et al. (2017b). In this approach, an LSTM recurrent network transforms the question q into biases β and element-wise multipliers γ : $[\gamma; \beta] = W \cdot LSTM(q) + b$. These so-called FiLM coefficients are then applied in the blocks of a deep residual convolutional network (He et al., 2016). A FiLM-ed residual block takes a tensor-valued input h_{in} and performs the following computation upon it:

$$\tilde{h} = BN(W_2 * R(W_1 * h_{in} \oplus b_1) \oplus b_2), \quad (5)$$

$$h_{out} = R(h_{in} + \gamma \odot \tilde{h} \oplus \beta), \quad (6)$$

where R stands for the Rectified Linear Unit, BN denotes batch normalization (Ioffe & Szegedy, 2015). Several such blocks are stacked together

and applied to a 3D feature tensor h_x that is produced by several layers of convolutions, some of them pretrained. The FiLM-ed network thus processes the input image x in a manner that is modulated by the question q . Despite its simplicity, FiLM achieves a remarkably high reported accuracy of 97.7% on the CLEVR task. A more advanced model that we include in our evaluation is Memory-Attention-Composition (MAC, see Appendix B for description) by Hudson & Manning (2018).

3.2 Modular and Symbolic Approaches

In addition to the end-to-end differentiable models, we experiment with methods based on intermediate structured symbolic meaning representations. We adhere to the common practice of using programs expressed in the CLEVR DSL as such representations, although in principle logical formulae or other formalisms from the field of formal semantics could be used for this purpose. If a symbolic *execution engine* for the programs is available, the task of VQA can be reduced to parsing the question and the image into a program and a symbolic scene representation respectively. This has already been proposed by Yi et al. (2018) under the name Neural-Symbolic VQA (NS-VQA) with a reported CLEVR accuracy of 99.8%. This excellent performance, however, is achieved by relying heavily on the prior knowledge about the task, meaning that applying NS-VQA in conditions other than CLEVR could require significantly more adaptation and data collection than needed for the more generic methods, such as FiLM and MAC.

Intermediate symbolic programs can also be used without apriori knowledge of the semantics of the symbols, in which case the execution engine for the programs is either fully or partially learned. In the Neural Module Network (NMN) paradigm, proposed by Andreas et al. (2016), the meanings of symbols are represented in the form of trainable neural modules. Given a program, the modules that correspond to the program’s symbols are retrieved and composed following the program’s structure. Formally, a program in CLEVR DSL can be represented as a (P, L, R) triple, where $P = (p_1, p_2, \dots, p_T)$ is the sequence of function tokens², $L = (l_1, \dots, l_T)$ and $R = (r_1, \dots, r_T)$ are the indices of the left and right arguments for

²In this work we treat composite functions like e.g. “filter_color[brown]” as standalone ones, not as “filter_color” parameterized by “brown”.

each function call respectively (some DSL functions only take one or zero arguments, in which case the respective r_i and l_i are undefined). Using this formalism, a step of the NMN computation can be expressed as follows:

$$h_i = \begin{cases} M_{p_i}(h_x), & \text{arity}(p_i) = 0, \\ M_{p_i}(h_x, h_{l_i}), & \text{arity}(p_i) = 1, \\ M_{p_i}(h_x, h_{l_i}, h_{r_i}), & \text{arity}(p_i) = 2. \end{cases} \quad (7)$$

Here, M_{p_i} is the neural module corresponding to the function token p_i and h_i is its output, while h_x is a tensor representing the image. Similar to MAC, the output h_T of the last module is fed to the classifier, after which the modules are jointly trained by backpropagating the classifier’s loss. To produce the programs for NMN training and usage a *program generator* can be pretrained with a small seed set of (question, program)-pairs and then finetuned, e.g. with REINFORCE (Hu et al., 2017; Johnson et al., 2017), on the rest of the dataset, using only (image, question, answer)-triplets as supervision. The programs produced by such a program generator can then be used at test time, meaning that after training the complete model takes the same inputs as end-to-end continuous models, such as FiLM and MAC.

The first NMN model that we consider is the one proposed by Johnson et al. (2017), in which residual blocks (He et al., 2016) are used as neural modules M_{p_i} . For example, modules corresponding to functions of arity 2, (such as e.g. “and”, “equal_color”, etc.), perform the following computation in their approach:

$$\tilde{h} = R(W_1 * [h_{l_i}; h_{r_i}]), \quad (8)$$

$$h_i = R(W_3 * R(W_2 * \tilde{h} \oplus b_2) \oplus b_3 + \tilde{h}). \quad (9)$$

Note that the module described above does not use the image representation h_x as an input; only the M_{scene} module—the root node in all CLEVR programs—does so.

Our preliminary experiments showed that such modules often perform much worse when assembled in novel combinations. We hypothesized that this could be due to the fact that high-capacity 3D tensors h_i are used in this model as the interface between modules. In order to test this hypothesis, we have designed a new module with a lower-dimensional vector output. We will henceforth refer to the module by Johnson et al. (2017) and our new module as **Tensor-NMN** and **Vector-NMN** respectively. The computation of our Vector-NMN

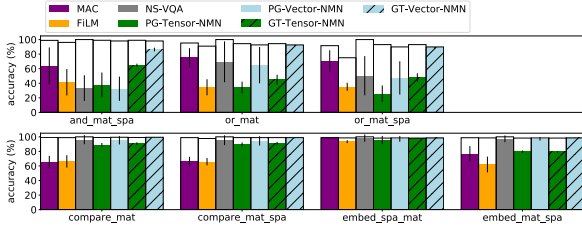


Figure 3: Zero-shot accuracy of all models on the 7 CLOSURE tests. For each model and test, the white bar in the background is the model’s accuracy on the closest CLEVR questions. The hatching used for “GT-...” models indicates that we used the ground-truth programs at test time.

is inspired by the FiLM approach to conditioning residual blocks on external inputs:

$$\tilde{h}_1 = R(U_1 * (\gamma_1 \odot h_x \oplus \beta_1)), \quad (10)$$

$$\tilde{h}_2 = R(U_2 * (\gamma_2 \odot \tilde{h}_1 \oplus \beta_2) + h_x), \quad (11)$$

$$h_i = \text{maxpool}(\tilde{h}_2), \quad (12)$$

where “maxpool” denotes max pooling of the 3D-tensor across all locations. Note that each Vector-NMN module also takes the image feature tensor h_x as the input, unlike Tensor-NMN. The above equations describe a 1-block version of Vector-NMN, but in general several FiLM-ed residual blocks described by Equations 10 and 11 can be stacked prior to the pooling. The FiLM coefficients β_1 , β_2 , γ_1 and γ_2 are computed by 1-hidden-layer MLPs from the concatenation $h_c = [e(p_i); h_{l_i}; h_{r_i}]$ of the embedding $e(p_i)$ of the function token p_i and the module inputs h_{l_i} and h_{r_i} :

$$[\beta_k, \tilde{\gamma}_k] = W_2^k (R(W_1^k h_c + b_1^k) + b_2^k), \quad (13)$$

$$\gamma_k = 2 \tanh(\tilde{\gamma}_k) + 1. \quad (14)$$

The tanh nonlinearity in Equation 14 was required to achieve stable training. Unlike in Tensor-NMN, the convolutional filters U_1 and U_2 are reused among all modules. To make this possible, we feed zero vectors instead of h_{r_i} or h_{l_i} when the function p_i takes less than two inputs.

4 Experiments

We use the original implementation for FiLM and Tensor-NMN and train these models with the hyperparameter settings suggested by the authors. For the MAC model, we use a reimplementation that is close to the original one. We report results for a 2-block version of Vector-NMN, as our preliminary experiments on the original CLEVR dataset

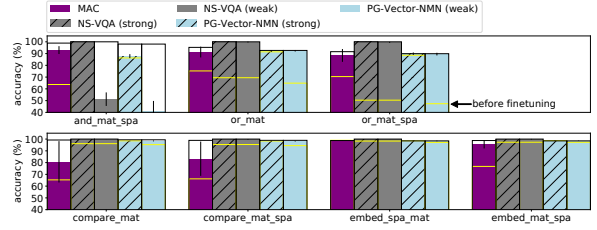


Figure 4: The accuracies for NS-VQA, PG-Vector-NMN and MAC after finetuning on 36 examples from each CLOSURE family. The background white bar is the model’s accuracy on the closest CLEVR questions. The hatching indicates the use of ground-truth programs at the fine-tuning stage.

showed that it performs better than the 1-block version. For all models that rely on symbolic programs, i.e. NS-VQA and the NMNs, we use a standard seq2seq model with an attention mechanism (Bahdanau et al., 2015) as the program generator. We report results for program generators trained with on the (question, program)-pairs from all 700k CLEVR examples. In addition to evaluating the NMNs with the predicted programs, we also measure their performance when the ground-truth programs are given at test time. For the latter setting, we prepend **GT** to the model’s name (as in GT-Vector-NMN), as opposed to prepending **PG** (as in PG-Vector-NMN). All numbers that we report are averages over 5 or 10 runs. Where relevant, we also report the standard deviation σ in the form of $\pm\sigma$ or as a vertical black bar in figures. A detailed tabular presentation of the results is available in Appendix C. For exact training settings and hyperparameters we refer the reader to Appendix G.

4.1 Zero-shot Generalization

In our first set of experiments, we assess zero-shot systematic generalization of models trained on CLEVR by measuring their performance on the CLOSURE tests. To put these results in context, for each model and test we measure the model’s performance on validation questions from CLEVR that are most similar to the given test’s questions. For example, consider the `embed_spa_mat` questions in which a spatial RE is embedded in a matching RE, such as “Is there a big blue metal thing that is the same shape as the rubber object behind the blue shiny object?”. To establish a baseline for this test, we used existence questions where a spatial RE was embedded in another spatial RE, such as “Is there a big blue metal thing that is behind the rub-

ber object behind the blue shiny object?” (notably, all models were accurate on $> 98\%$ of such questions). The gap between the model’s performance on baseline questions and the model’s performance on a CLOSURE test is indicative of how systematic the model’s generalization behavior is. See Appendix F for more details on baseline questions.

The results are reported in Figure 3. One can clearly see that most models perform significantly worse on most CLOSURE tests compared to their accuracies on the respective baseline questions. A notable exception is `embed_spa_mat`, on which all models perform quite well. Among generic models, MAC consistently fares better than FiLM, albeit the former still loses 15% to 35% of its baseline accuracy in 6 out of 7 tests. Surprisingly, the NS-VQA model, whose only learnable component is a program generator, generalizes outright badly on tests that involved logical references, and also shows significant deterioration compared to baseline questions on other tests. This lack of systematic generalization in program generation also strongly affects performances of the two NMN models that we considered (PG-Vector-NMN and PG-Tensor-NMN). Interestingly, even given the ground-truth programs at test-time, Tensor-NMN modules perform worse on CLOSURE questions than on the respective baseline questions in 6 tests out of 7 (see GT-Tensor-NMN results). In contrast, our proposed Vector-NMN module generalizes much better, matching its baseline performance almost always, with a notable exception of the `and_mat_spa` test. We conduct an additional investigation to better understand why Vector-NMN outperforms Tensor-NMN. These extra results (Appendix H) suggest that the max-pooling operation, which turns the Vector-NMN’s output from a tensor into a vector, plays a key role in the module’s improved generalization performance.

4.2 Few-shot transfer learning

The results above show that inductive biases of existing models are often insufficient for zero-shot systematic generalization measured by CLOSURE. A natural question to ask in these circumstances is whether just a few examples would be sufficient to correct the models’ extrapolation behavior. To answer this question, we finetune MAC, PG-Vector-NMN and NS-VQA models that are pretrained on CLEVR using 36 examples from each CLOSURE family, for a total of 252 new examples. For PG-

Vector-NMN and NS-VQA we consider two finetuning scenarios: one where the programs are provided for new examples and one where they are not given and must be inferred. To infer programs, we use a basic REINFORCE-based program induction approach (Johnson et al., 2017; Hu et al., 2017). We will refer to the two said scenarios as strong and weak supervision respectively. To get the best finetuning performance, we oversample 300 times the 252 training CLOSURE examples, add them to the CLEVR training set and train on the resulting mixed dataset. Just like in zero-shot experiments, we consider the model’s performance on the closest CLEVR questions as the systematic generalization target.

The few-shot results, reported in Figure 4, show that as few as 36 examples from each family can significantly improve CLOSURE performance for all models. A notable exception from this general observation is the `and_mat_spa` question family, on which weakly supervised program induction for NS-VQA and PG-Vector-NMN most often did not work. We analyzed this case in detail and found that the appropriate programs for `and_mat_spa` would typically have a very low probability, and hence were never sampled in our REINFORCE-based program search.

The impact of 36 examples varies widely depending on the model and test. Models using symbolic programs reached the target performance in 6 tests out of 7. On the contrary, for MAC a gap of 5% to 20% between its CLOSURE and target accuracies remained on all tests, except for the `embed_spa_mat` test that MAC handled well even without fine-tuning. Notably, unlike the models relying on weakly-supervised program induction, MAC benefited greatly from fine-tuning on the challenging `and_mat_spa` test. Besides, MAC’s and PG-Vector-NMN’s absolute performance on `or_mat` and `or_mat_spa` are comparable.

5 Related Work

Several related generalization tests that were proposed for CLEVR and other VQA datasets differ from CLOSURE in what they aim to measure and/or how they were constructed. The Compositional Generalization Test (CoGenT) from the original paper by Johnson et al. (2016) restricts the colors that cubes and cylinders can have in the training set images and inverts this restriction during the test time. By its design, CoGenT evalu-

ates how robust a model is to a shift in the image distribution. On the contrary, in CLOSURE the image distribution remains the same at test time, but the question distribution changes to contain novel combinations of linguistic constructs from CLEVR. The generalization splits from the Shape-World platform (Kuhle & Copestake, 2017) also focus on the difference in the distribution of images, not questions. The CLEVR-Humans dataset was collected by having crowd workers ask questions about CLEVR images (Johnson et al., 2017). Some questions from this dataset require reasoning that is outside of the scope of CLEVR, such as e.g. quantification (“Are all the balls small?”). In contrast, CLOSURE requires models to recombine only the well-known reasoning primitives. A compositional C-VQA split was proposed for the VQA 1.0 dataset (Agrawal et al., 2017). In C-VQA similar questions must have different answers when they appear in the training and test sets, yet the distributions of questions at training and testing remain similar, unlike CLOSURE.

Perhaps the closest to our work is the SGOOP dataset and the study conducted on it by Bahdanau et al. (2019). SGOOP features questions of the form “Is there an X R of Y”, where X and Y are object words and R a spatial relation. The authors test whether models can answer all possible SGOOP questions after training on a subset that is defined by holding out most of the (X, Y) pairs. The methodology of that study is thus very similar to ours, however the specific nature of the generalization split is different. Similarly to our results, Bahdanau et al. (2019) report significant generalization gaps for a number of VQA models, with a notable exception of the Tensor-NMN, that generalized perfectly in their study when a tree-like layout was used to connect the modules. We believe our CLOSURE results are an important addition to the SGOOP ones. The specific cause of the aforementioned discrepancies between the two studies is, however, an intriguing question for future work.

As can be clearly seen from the performance of the NS-VQA model, much of the performance drop that we reported can be explained by insufficient systematicity of seq2seq models that we use for program generation. The SCAN dataset (Lake & Baroni, 2018) and the follow-up works (Loula et al., 2018; Bastings et al., 2018) have recently brought much-needed attention to this important issue. Compared to SCAN, CLOSURE

features richer and more natural-looking language, and hence can serve to validate the conclusions drawn in recent SCAN-based studies, e.g. (Russin et al., 2019). Concurrently to this work, (Hupkes et al., 2019) and (Keyzers et al., 2020) developed related benchmarks that also test systematicity of neural seq2seq transducers.

Prior work on NMNs features modules that output either attention maps (Andreas et al., 2016; Hu et al., 2017, 2018) or feature tensors (Johnson et al., 2017). The model by (Mascharka et al., 2018) combines modules with both attention- and tensor-valued outputs. Our Vector-NMN generalizes more systematically than its tensor-based predecessor by Johnson et al. (2017), while inheriting that model’s simplicity, generality and good CLEVR performance.

6 Discussion

Our study shows that while models trained on CLEVR are very good at answering questions from CLEVR, their high performance quickly deteriorates when the question distribution features unfamiliar combinations of well-known primitives. We believe that this is an interesting finding, given that CLEVR puts VQA models in very favorable conditions: the training set is large and well-balanced and complex questions are well represented.

While in our zero-shot test of systematic generalization all models fare similarly badly, our few-shot learning study highlights important differences in their behavior. Given few examples, the program-based models either almost perfectly adapt to the target task or completely fail, depending on whether the right programs are found. For end-to-end continuous models back-propagation is always effective in adapting them to the target examples, but the systematic generalization gap is often not fully bridged with a number of examples that is sufficient for the program-based models. An important context for this comparison is that program-based models require seed programs to jump-start the training and are later on constrained to the seed lexicon. It would be highly desirable to combine the strengths of these two types of systems in one model without inheriting any of their limitations, a direction that we would like to explore in our future work.

References

- Agrawal, A., Batra, D., and Parikh, D. Analyzing the Behavior of Visual Question Answering Models. In *Proceedings of the 2016 Conference on Empirical Methods in Natural Language Processing*, January 2016.
- Agrawal, A., Kembhavi, A., Batra, D., and Parikh, D. C-VQA: A Compositional Split of the Visual Question Answering (VQA) v1.0 Dataset. *arXiv:1704.08243 [cs]*, April 2017. URL <http://arxiv.org/abs/1704.08243>. arXiv: 1704.08243.
- Andreas, J., Rohrbach, M., Darrell, T., and Klein, D. Neural Module Networks. In *Proceedings of 2016 IEEE Conference on Computer Vision and Pattern Recognition (CVPR)*, 2016. URL <http://arxiv.org/abs/1511.02799>.
- Antol, S., Agrawal, A., Lu, J., Mitchell, M., Batra, D., Lawrence Zitnick, C., and Parikh, D. Vqa: Visual Question Answering. In *Proceedings of the 2015 IEEE International Conference on Computer Vision (CVPR)*, pp. 2425–2433, 2015.
- Bahdanau, D., Cho, K., and Bengio, Y. Neural Machine Translation by Jointly Learning to Align and Translate. In *International Conference on Learning Representations, ICLR 2015*, 2015.
- Bahdanau, D., Murty, S., Noukhovitch, M., Nguyen, T. H., Vries, H. d., and Courville, A. Systematic Generalization: What Is Required and Can It Be Learned? In *International Conference on Learning Representations, ICLR 2019*, 2019. URL <https://openreview.net/forum?id=HkezXnA9YX>.
- Bastings, J., Baroni, M., Weston, J., Cho, K., and Kiela, D. Jump to better conclusions: SCAN both left and right. In *Proceedings of the 2018 EMNLP Workshop BlackboxNLP: Analyzing and Interpreting Neural Networks for NLP*. Association for Computational Linguistics, November 2018. URL <https://www.aclweb.org/anthology/W18-5407>.
- Fodor, J. A. and Pylyshyn, Z. W. Connectionism and cognitive architecture: A critical analysis. *Cognition*, 28(1):3–71, 1988.
- He, K., Zhang, X., Ren, S., and Sun, J. Deep residual learning for image recognition. In *Proceedings of the IEEE Conference on Computer Vision and Pattern Recognition*, 2016.
- Hu, R., Andreas, J., Rohrbach, M., Darrell, T., and Saenko, K. Learning to Reason: End-to-End Module Networks for Visual Question Answering. In *Proceedings of 2017 IEEE International Conference on Computer Vision*, April 2017. URL <http://arxiv.org/abs/1704.05526>. arXiv: 1704.05526.
- Hu, R., Andreas, J., Darrell, T., and Saenko, K. Explainable Neural Computation via Stack Neural Module Networks. In *arXiv:1807.08556 [cs]*, July 2018. URL <http://arxiv.org/abs/1807.08556>. arXiv: 1807.08556.
- Hudson, D. A. and Manning, C. D. Compositional Attention Networks for Machine Reasoning. In *Proceedings of the 2018 International Conference on Learning Representations*, February 2018. URL <https://openreview.net/forum?id=S1Euwz-Rb>.
- Hupkes, D., Dankers, V., Mul, M., and Bruni, E. The compositionality of neural networks: integrating symbolism and connectionism. *arXiv:1908.08351 [cs, stat]*, August 2019. URL <http://arxiv.org/abs/1908.08351>. arXiv: 1908.08351.
- Ioffe, S. and Szegedy, C. Batch Normalization: Accelerating Deep Network Training by Reducing Internal Covariate Shift. In *Proceedings of the 32nd International Conference on Machine Learning, ICML 2015*, 2015. URL <http://jmlr.org/proceedings/papers/v37/ioffe15.html>.
- Johnson, J., Hariharan, B., van der Maaten, L., Fei-Fei, L., Zitnick, C. L., and Girshick, R. CLEVR: A Diagnostic Dataset for Compositional Language and Elementary Visual Reasoning. In *Proceedings of 2017 IEEE Conference on Computer Vision and Pattern Recognition (CVPR)*, December 2016. arXiv: 1612.06890.
- Johnson, J., Hariharan, B., van der Maaten, L., Hoffman, J., Fei-Fei, L., Zitnick, C. L., and Girshick, R. Inferring and Executing Programs for Visual Reasoning. In *Proceedings of 2017 IEEE International Conference on Computer Vision, ICCV 2017*, 2017. URL <http://arxiv.org/abs/1705.03633>.
- Keyzers, D., Schärli, N., Scales, N., Buisman, H., Furrer, D., Kashubin, S., Momchev, N., Sinopalnikov, D., Stafiniak, L., Tihon, T., Tsarkov, D., Wang, X., van Zee, M., and Bousquet, O. Measuring Compositional Generalization: A Comprehensive Method on Realistic Data. In *International Conference on Learning Representations*, 2020. arXiv: 1912.09713.
- Kingma, D. P. and Ba, J. Adam: A Method for Stochastic Optimization. In *Proceedings of the 2015 International Conference on Learning Representations, ICLR 2015*, 2015. URL <http://arxiv.org/abs/1412.6980>. arXiv: 1412.6980.
- Kuhnle, A. and Copestake, A. ShapeWorld - A new test methodology for multimodal language understanding. *arXiv:1704.04517 [cs]*, April 2017. URL <http://arxiv.org/abs/1704.04517>. arXiv: 1704.04517.
- Lake, B. M. and Baroni, M. Generalization without systematicity: On the compositional skills of sequence-to-sequence recurrent networks. In *Proceedings of the 36th International Conference on*

- Machine Learning*, 2018. URL <http://arxiv.org/abs/1711.00350>. arXiv: 1711.00350.
- Loula, J., Baroni, M., and Lake, B. M. Rearranging the Familiar: Testing Compositional Generalization in Recurrent Networks. In *Proceedings of the 2018 BlackboxNLP EMNLP Workshop*, July 2018. URL <https://arxiv.org/abs/1807.07545>.
- Mascharka, D., Tran, P., Soklaski, R., and Majumdar, A. Transparency by Design: Closing the Gap Between Performance and Interpretability in Visual Reasoning. In *2018 IEEE Conference on Computer Vision and Pattern Recognition*, March 2018. URL <http://arxiv.org/abs/1803.05268>. arXiv: 1803.05268.
- Perez, E., de Vries, H., Strub, F., Dumoulin, V., and Courville, A. Learning Visual Reasoning Without Strong Priors. *arXiv:1707.03017 [cs, stat]*, July 2017a. URL <http://arxiv.org/abs/1707.03017>. arXiv: 1707.03017.
- Perez, E., Strub, F., de Vries, H., Dumoulin, V., and Courville, A. FiLM: Visual Reasoning with a General Conditioning Layer. In *In Proceedings of the 2017 AAAI Conference on Artificial Intelligence*, 2017b. URL <http://arxiv.org/abs/1709.07871>.
- Russin, J., Jo, J., and O’Reilly, R. C. Compositional generalization in a deep seq2seq model by separating syntax and semantics. *arXiv:1904.09708 [cs, stat]*, April 2019. URL <http://arxiv.org/abs/1904.09708>. arXiv: 1904.09708.
- Santoro, A., Raposo, D., Barrett, D. G. T., Malinowski, M., Pascanu, R., Battaglia, P., and Lillicrap, T. A simple neural network module for relational reasoning. In *Advances in Neural Information Processing Systems 31*, June 2017. URL <http://arxiv.org/abs/1706.01427>. arXiv: 1706.01427.
- Sutskever, I., Vinyals, O., and Le, Q. V. Sequence to Sequence Learning with Neural Networks. In *Advances in Neural Information Processing Systems 27*, pp. 3104–3112, 2014.
- Yi, K., Wu, J., Gan, C., Torralba, A., Kohli, P., and Tenenbaum, J. B. Neural-Symbolic VQA: Disentangling Reasoning from Vision and Language Understanding. *Advances in Neural Information Processing Systems 31: NeurIPS 2018*, October 2018. URL <http://arxiv.org/abs/1810.02338>. arXiv: 1810.02338.

A The CLEVR DSL and CLOSURE Programs Expressed In It

The DSL functions that implement meanings of referring expressions operate on sets of objects, where each object is represented by the values of its four properties (shape, color, size and material) and its spatial coordinates. *Filter* functions filter the input set of objects by the value of a property (e.g. “filter_color[brown]”, “filter_shape[cube]”), and *relations* return a set of all other objects that are related to the given object. The two kinds of relations in the DSL correspond to the spatial and matching predicates that we discussed above. Namely, there are spatial relations: (“relate[left]”, “relate[right]”, ...) and matching relations (“same_shape”, “same_color”, ...). The subprograms that correspond to the REs consist of chained filters and relations, as well as set union and set intersection functions in the case of logical REs³. The wider use of matching predicates that distinguishes CLOSURE questions from CLEVR ones translates into matching relations appearing in more diverse kinds of programs than in CLEVR. For example, in program P3 in Figure 2 the relation “same_size” appears in the same program with the function “equal_color”, a combination that would not be possible in CLEVR. Hence, to succeed on CLOSURE, the NMN models have to learn modules which can be arbitrarily recombined with each other.

B Memory-Attention-Composition (MAC) Model

In the MAC approach by (Hudson & Manning, 2018), the input and control components of the model first produce a sequence of control vectors c_i from the question q . A visual attention component (called the read unit in the original paper) is then recurrently applied to a preprocessed version h_x of the image x . The i -th application of the read unit is conditioned on the respective control vector c_i and on a memory m_i of the unit’s outputs at the previous steps:

C Tabular CLOSURE Results

See Table 1 for zero-shot results, Table 2 for few-shot results, and Table 3 for the target performances for all CLOSURE tests.

model	and_mat_spa	or_mat	or_mat_spa
FiLM	41.4 ± 18	34.4 ± 11	35.2 ± 5.5
MAC	63.7 ± 25	75.2 ± 13	70.4 ± 15
NS-VQA	33.3 ± 18	69.5 ± 28	50.4 ± 27
PG-Tensor-NMN	37.6 ± 17	34.1 ± 8.1	25.5 ± 11
PG-Vector-NMN	32.5 ± 17	64.9 ± 25	47.4 ± 23
GT-Tensor-NMN	64.9 ± 2	44.8 ± 6.8	47.9 ± 5.8
GT-Vector-NMN	86.3 ± 2.5	91.5 ± 0.77	88.6 ± 1.2

model	embed_spa_mat	embed_mat_spa	compare_mat	compare_mat_spa
FiLM	93.4 ± 2	62 ± 11	66.2 ± 8.5	65.8 ± 5
MAC	99 ± 0.15	76.8 ± 11	65.3 ± 8.6	66.2 ± 6.4
NS-VQA	98.3 ± 5	97.3 ± 4.6	96.1 ± 6.2	95.4 ± 6.7
PG-Tensor-NMN	95.6 ± 5.6	79.8 ± 1.4	89.2 ± 2.3	89.8 ± 2.7
PG-Vector-NMN	97.2 ± 3.9	97.3 ± 2.4	95.3 ± 5.7	94.4 ± 6.4
GT-Tensor-NMN	98.1 ± 0.38	79.3 ± 0.83	90.7 ± 1.8	91.2 ± 1.9
GT-Vector-NMN	98.5 ± 0.13	98.7 ± 0.19	98.5 ± 0.17	98.4 ± 0.3

Table 1: Zero-shot performance of all models on CLOSURE tests. Reported is the mean accuracy and its standard deviation.

³The “unique” function also frequently appears in the subprograms that correspond to REs. Its only role is to raise an exception if its input is not a singleton set.

model	and_mat_spa	or_mat	or_mat_spa
NS-VQA (strong)	100	100 ± 0.026	100 ± 0.079
NS-VQA (weak)	51.2 ± 5.8	99.8 ± 0.38	99.5 ± 0.42
PG-Vector-NMN (strong)	87.8 ± 1.7	92.3 ± 0.68	89.9 ± 1
PG-Vector-NMN(weak)	40.8 ± 8.9	92.4 ± 0.65	89.5 ± 1.1
MAC	93 ± 3.3	91.3 ± 4.6	88.4 ± 5.5

model	embed_spa_mat	embed_mat_spa	compare_mat	compare_mat_spa
NS-VQA (strong)	100	100	100	100
NS-VQA (weak)	100 ± 0.026	99.9 ± 0.24	100 ± 0.034	99.8 ± 0.24
PG-Vector-NMN (strong)	98.5 ± 0.21	98.5 ± 0.26	98.3 ± 0.29	98.3 ± 0.31
PG-Vector-NMN(weak)	98.4 ± 0.26	98.5 ± 0.17	98.4 ± 0.37	98.2 ± 0.29
MAC	99 ± 0.12	95.6 ± 3.6	80.7 ± 18	83.3 ± 15

Table 2: Performance of several models on CLOSURE tests after finetuning on 252 CLOSURE examples, 36 from each family. Reported is the mean accuracy and its standard deviation.

D Results for the original MAC implementation

To validate our conclusions, we also tried to measure performance of the reference MAC implementation by Hudson & Manning (2018) on CLOSURE tests. We ran the codes 10 times using the default configuration. The results are reported in Table 4. While some accuracy differences are statistical significant (e.g. `or_mat`), these results would lead to same conclusions as the ones that we obtained by using the approximate reimplementation by Bahdanau et al. (2019). The latter was more convenient for us to use because it is written using the framework that we use for all other models, namely PyTorch.

E CLEVR results

In Table 5 we report the accuracies on the CLEVR validation test for all the models that we consider in this study (including the ones introduced below in Appendix H).

F Further details on CLOSURE and baseline questions

The exact CLOSURE templates can be found in Figure 5. The templates for the baseline questions, that is CLEVR questions that are most similar to CLOSURE ones, can be found in Figure 6. The slots in the templates should be understood as follows:

- the slots $\langle A \rangle$ and $\langle Q \rangle$ will be filled by names of CLEVR properties, such as “shape”, “size”, “color” and “material”
- the slots $\langle Z \rangle$, $\langle C \rangle$, $\langle M \rangle$ and $\langle S \rangle$ will be either left blank or filled by words that characterize objects’ properties, such as “big”, “small”, “yellow”, “rubber”, “cube”, etc.
- the $\langle R \rangle$ slots will be filled with spatial words, such as “left of”, “right of”, “behind” or “in front of”.

In some templates fragments of text are in square brackets; those are optional and will be discarded with 50% probability.

We generate the questions from the templates in two stages. At the first stage, we fill the $\langle A \rangle$ and $\langle Q \rangle$ slots, and at the second stage we use CLEVR question generation code to fill the rest. The two-stage procedure is required because the original generation engine does not support $\langle A \rangle$ and $\langle Q \rangle$ slots; instead, CLEVR authors wrote unique templates for each property that is queried (the purpose of $\langle Q \rangle$) or used to refer to objects (the purpose of $\langle A \rangle$).

We used CLEVR generation code mostly as is, with the exception of two important modifications. First, we restricted the answers of counting questions to be either 1, 2 or 3, and also applied more aggressive

model	and_mat_spa	or_mat	or_mat_spa
MAC	98.9 ± 0.35	95.3 ± 0.62	91.6 ± 2.6
FiLM	96.1 ± 1.6	91 ± 0.99	75 ± 2.1
NS-VQA	100	100 ± 0.0088	100
PG-Tensor-NMN	99 ± 0.3	94.4 ± 0.67	93.1 ± 0.62
PG-Vector-NMN	98.1 ± 0.33	92.7 ± 1.1	89.9 ± 1.3
GT-Tensor-NMN	99 ± 0.3	94.4 ± 0.67	93.1 ± 0.62
GT-Vector-NMN	98.1 ± 0.33	92.7 ± 1.1	89.9 ± 1.3

model	embed_spa_mat	embed_mat_spa	compare_mat	compare_mat_spa
MAC	98.8 ± 0.56	98.8 ± 0.56	99.2 ± 0.15	98.9 ± 0.27
FiLM	98.5 ± 0.54	98.5 ± 0.54	98.9 ± 0.39	97.7 ± 0.76
NS-VQA	100	100	100	100
PG-Tensor-NMN	98.3 ± 0.81	98.3 ± 0.81	99.2 ± 0.32	98.9 ± 0.17
PG-Vector-NMN	98.5 ± 0.53	98.5 ± 0.53	99.4 ± 0.17	98.9 ± 0.24
GT-Tensor-NMN	98.3 ± 0.81	98.3 ± 0.81	99.2 ± 0.32	98.9 ± 0.17
GT-Vector-NMN	98.5 ± 0.53	98.5 ± 0.53	99.4 ± 0.17	98.9 ± 0.24

Table 3: Models’ performance on CLEVR questions that are the closest to a given CLOSURE test (see Appendix F for additional details regarding the closest questions for `or_mat` and `or_mat_spa`). Reported is the mean accuracy and its standard deviation.

model	and_mat_spa	or_mat	or_mat_spa
reimpl. by (Bahdanau et al., 2019)	63.7 ± 25	75.2 ± 13	70.4 ± 15
original by (Hudson & Manning, 2018)	77.1 ± 11	57.8 ± 7.7	55.3 ± 6.3

model	embed_spa_mat	embed_mat_spa	compare_mat	compare_mat_spa
reimpl. by (Bahdanau et al., 2019)	99 ± 0.15	76.8 ± 11	65.3 ± 8.6	66.2 ± 6.4
original by (Hudson & Manning, 2018)	98.6 ± 0.89	69.5 ± 7.5	65.1 ± 5.3	64.3 ± 3.1

Table 4: Comparison between CLOSURE accuracies of two MAC implementation, the original one by Hudson & Manning (2018), and the reimplementation by Bahdanau et al. (2019)

rejection sampling to make these answers equally likely. We did so because the distribution of answers to counting questions in CLEVR is skewed, and answers of 4 and more are very unlikely. Instead of trying to replicate the original skewed answer distribution, we chose to enforce uniformity among those answers (that is 1, 2 and 3) that do have a significant probability in CLEVR. We did not allow 0 as the answer because due to implementation details, CLEVR questions that contain logical “or” and a complex spatial RE never have 0 as the answer. Overall, with our modifications to generation of counting questions we tried to put side the irrelevant confounding factors and focus on the impact of replacing a spatial RE with a matching one. To compute the appropriate target performance for `or_mat` and `or_mat_spa`, we generated new questions from the closest original CLEVR templates but using the modified version of the generation code.

The second modification concerns the question degeneracy check that is described in the appendix of (Johnson et al., 2016). In the reference question generation code it is only applied to programs with spatial relations. We modified the code to also apply the degeneracy check to matching relations.

A minor issue with `compare_mat` and `compare_mat_spa` questions is that the word “another” can be used in cases where it is not required, e.g. “... another cube that is the same size as the sphere”. CLEVR generation code removes “another” in such cases, but we found it hard to extend this feature to CLOSURE questions in a maintainable way. In our preliminary experiments we found the proper handling of “another” does not change results of zero-shot experiments. We also experimented with removing the word “is”

model	CLEVR accuracy
MAC	98.5 \pm 0.11
FiLM	97 \pm 0.56
NS-VQA	100 \pm 0.00021
PG-Tensor-NMN	97.9 \pm 0.052
PG-Vector-NMN	98 \pm 0.066
GT-Tensor-NMN	97.9 \pm 0.052
GT-Vector-NMN	98 \pm 0.066
GT-Tensor-NMN-Shortcuts	98 \pm 0.079
GT-Tensor-NMN-FiLM	94.8 \pm 1.7

Table 5: CLEVR validation accuracies for all models

- **embed_spa_mat** Is there a $\langle Z \rangle \langle C \rangle \langle M \rangle \langle S \rangle$ that is the same $\langle A \rangle$ as the $\langle Z2 \rangle \langle C2 \rangle \langle M2 \rangle \langle S2 \rangle \langle R \rangle$ the $\langle Z3 \rangle \langle C3 \rangle \langle M3 \rangle \langle S3 \rangle$?
- **embed_mat_spa** Is there a $\langle Z \rangle \langle C \rangle \langle M \rangle \langle S \rangle \langle R \rangle$ the $\langle Z2 \rangle \langle C2 \rangle \langle M2 \rangle \langle S2 \rangle$ that is the same $\langle A \rangle$ as $\langle Z3 \rangle \langle C3 \rangle \langle M3 \rangle \langle S3 \rangle$?
- **compare_mat** There is another $\langle Z \rangle \langle C \rangle \langle M \rangle \langle S \rangle$ that is the same $\langle A \rangle$ as the $\langle Z2 \rangle \langle C2 \rangle \langle M2 \rangle \langle S2 \rangle$; does it have the same $\langle Q \rangle$ as the $\langle Z3 \rangle \langle C3 \rangle \langle M3 \rangle \langle S3 \rangle$?
- **compare_mat_spa** There is another $\langle Z \rangle \langle C \rangle \langle M \rangle \langle S \rangle$ that is the same $\langle A \rangle$ as the $\langle Z2 \rangle \langle C2 \rangle \langle M2 \rangle \langle S2 \rangle$; does it have the same $\langle Q \rangle$ as the $\langle Z3 \rangle \langle C3 \rangle \langle M3 \rangle \langle S3 \rangle$ [that is] $\langle R2 \rangle$ the $\langle Z4 \rangle \langle C4 \rangle \langle M4 \rangle \langle S4 \rangle$?
- **and_mat_spa** What is the $\langle Q \rangle$ of the $\langle Z \rangle \langle C \rangle \langle M \rangle \langle S \rangle$ that is $\langle R2 \rangle$ the $\langle Z2 \rangle \langle C2 \rangle \langle M2 \rangle \langle S2 \rangle$ and is the same $\langle A \rangle$ as the $\langle Z3 \rangle \langle C3 \rangle \langle M3 \rangle \langle S3 \rangle$?
- **or_mat** How many things are [either] $\langle Z \rangle \langle C \rangle \langle M \rangle \langle S \rangle$ s or $\langle Z2 \rangle \langle C2 \rangle \langle M2 \rangle \langle S2 \rangle$ s that are the same $\langle A \rangle$ as the $\langle Z3 \rangle \langle C3 \rangle \langle M3 \rangle \langle S3 \rangle$?
- **or_mat_spa** How many things are [either] $\langle Z \rangle \langle C \rangle \langle M \rangle \langle S \rangle$ s [that are] $\langle R \rangle$ the $\langle Z2 \rangle \langle C2 \rangle \langle M2 \rangle \langle S2 \rangle$ or $\langle Z3 \rangle \langle C3 \rangle \langle M3 \rangle \langle S3 \rangle$ s that are the same $\langle A \rangle$ as the $\langle Z4 \rangle \langle C4 \rangle \langle M4 \rangle \langle S4 \rangle$?

Figure 5: CLOSURE templates.

from “... and is the same $\langle A \rangle$...” in the `and_mat_spa` template to make it more similar to the closest CLEVR questions, in which “and” combines prepositional phrases (i.e. “... that is left of the cube and right of the sphere”). Likewise, we saw no influence on the zero-shot results.

G Training Details

We train all models using the Adam optimizer (Kingma & Ba, 2015) with the hyperparameters $\beta_1 = 0.9$, $\beta_2 = 0.999$, $\epsilon = 10^{-8}$. The learning rate, the weight decay and the batch size varied across models, the exact values can be found in Table 6.

H Vector-NMN

See Figure 8 for a visual explanation of the Vector-NMN architecture.

We conducted additional experiments to better understand why Vector-NMN outperforms Tensor-NMN. First, we considered a module architecture that differs from Tensor-NMN in that every module takes the image representation h_x as an additional input. We called this model Tensor-NMN-Shortcut. Second, we evaluated a module architecture that is similar to Vector-NMN, but in which the module output h_i is not max-pooled and remains a 3D tensor. To feed h_i as an input to downstream modules, we concatenated

- **embed_spa_mat** Is there a ⟨Z⟩ ⟨C⟩ ⟨M⟩ ⟨S⟩ [that is] ⟨R⟩ the ⟨Z2⟩ ⟨C2⟩ ⟨M2⟩ ⟨S2⟩ [that is] ⟨R2⟩ the ⟨Z3⟩ ⟨C3⟩ ⟨M3⟩ ⟨S3⟩?
- **embed_mat_spa** Is there a ⟨Z⟩ ⟨C⟩ ⟨M⟩ ⟨S⟩ [that is] ⟨R⟩ the ⟨Z2⟩ ⟨C2⟩ ⟨M2⟩ ⟨S2⟩ [that is] ⟨R2⟩ the ⟨Z3⟩ ⟨C3⟩ ⟨M3⟩ ⟨S3⟩?
- **compare_mat** There is a ⟨Z⟩ ⟨C⟩ ⟨M⟩ ⟨S⟩ [that is] ⟨R⟩ the ⟨Z2⟩ ⟨C2⟩ ⟨M2⟩ ⟨S2⟩; does it have the same ⟨Q⟩ as the ⟨Z3⟩ ⟨C3⟩ ⟨M3⟩ ⟨S3⟩?
- **compare_mat_spa** There is a ⟨Z⟩ ⟨C⟩ ⟨M⟩ ⟨S⟩ [that is] ⟨R⟩ the ⟨Z2⟩ ⟨C2⟩ ⟨M2⟩ ⟨S2⟩; does it have the same ⟨Q⟩ as the ⟨Z3⟩ ⟨C3⟩ ⟨M3⟩ ⟨S3⟩ [that is] ⟨R2⟩ the ⟨Z4⟩ ⟨C4⟩ ⟨M4⟩ ⟨S4⟩?
- **and_mat_spa** What is the ⟨Q⟩ of the ⟨Z⟩ ⟨C⟩ ⟨M⟩ ⟨S⟩ that is [both] ⟨R⟩ the ⟨Z2⟩ ⟨C2⟩ ⟨M2⟩ ⟨S2⟩ and ⟨R2⟩ the ⟨Z3⟩ ⟨C3⟩ ⟨M3⟩ ⟨S3⟩?
- **or_mat** How many things are [either] ⟨Z⟩ ⟨C⟩ ⟨M⟩ ⟨S⟩s or ⟨Z2⟩ ⟨C2⟩ ⟨M2⟩ ⟨S2⟩s [that are] ⟨R⟩ the ⟨Z3⟩ ⟨C3⟩ ⟨M3⟩ ⟨S3⟩?
- **or_mat_spa** How many things are [either] ⟨Z⟩ ⟨C⟩ ⟨M⟩ ⟨S⟩s [that are] ⟨R⟩ the ⟨Z2⟩ ⟨C2⟩ ⟨M2⟩ ⟨S2⟩ or ⟨Z3⟩ ⟨C3⟩ ⟨M3⟩ ⟨S3⟩s [that are] ⟨R2⟩ the ⟨Z4⟩ ⟨C4⟩ ⟨M4⟩ ⟨S4⟩?

Figure 6: Baseline CLEVR templates.

model	learning rate	weight decay	batch size	training iterations	# of runs
MAC	10^{-4}	10^{-5}	64	1000000	10
FiLM	$3 \cdot 10^{-4}$	10^{-5}	64	500000	5
Tensor-NMN	10^{-4}	0	64	500000	5
Vector-NMN	10^{-4}	0	128	500000	10
PG	$7 \cdot 10^{-4}$	0	64	100000	10
PG (REINFORCE)	10^{-5}	0	128	200000	10

Table 6: Key hyperparameters and training settings. “PG” stands for the program generator that we used in PG-Vector-NMN and PG-Tensor-NMN, as well as in the NS-VQA model. The “PG (REINFORCE)” row contains the hyperparameters that we used to fine-tune the program generator on CLOSURE examples. For explanation of other acronyms, see Section 3 in the main text.

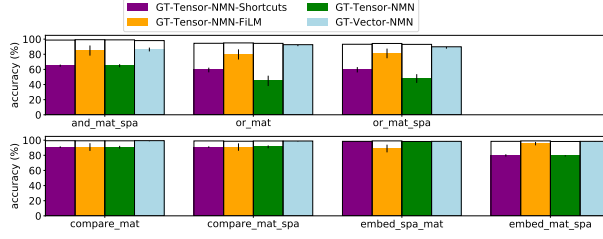


Figure 7: Comparing different module architectures. See Appendix H for more information.

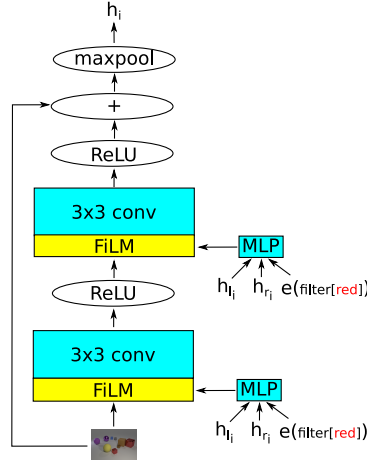


Figure 8: Computation performed by the Vector-NMN module. The 3D tensor h_x represents the input image x . h_{l_i} and h_{r_i} are the outputs of the two preceding modules l_i and r_i respectively. $e(p_i)$ is an embedding of the i -th program token. The weights of all matrix multiplications and convolutions (in cyan) are shared across all modules, whereas the unit-wise FiLM coefficients (in yellow) depend on the program token p_i that the i -th module corresponds to.

it to the image representation h_x in the same way as it is done in Tensor-NMN-Shortcut (note, that in Vector-NMN the pooled h_i would instead be used to compute FiLM coefficients of the downstream module). We will refer to this model as Tensor-NMN-FiLM. These two additional module architectures, namely Tensor-NMN-Shortcut and Tensor-NMN-FiLM, allow us to test whether just connecting every module to the image representation (the former) or sharing weights across modules (the latter) would alone be sufficient to achieve generalization comparable to that of Vector-NMN.

The results are reported in Figure 7. Both Tensor-NMN-Shortcut and Tensor-NMN-FiLM fall short of achieving their target performances on CLOSURE tests. This suggests that max-pooling the tensor-shaped module output and thereby turning it into a vector is indeed a key cause of the Vector-NMN’s better generalization.